



On the Onset of Taylor Vortices in Finite-Length Cavity Subject to a Radial Oscillation Motion

A. Lalaoua[†] and A. Bouabdallah

Faculty of Physic, Laboratory of Thermodynamics and Energetic Systems, USTHB, Bp 32, El alia, Algiers, Algeria.

[†]Corresponding Author Email: lalaouaaadel@gmail.com

(Received July 6, 2015; accepted August 22, 2015)

ABSTRACT

Taylor- Couette flow (TCF) is an important template for studying various mechanisms of the laminar-turbulent transition of rotating fluid in enclosed cavity. It is also relevant to engineering applications like bearings, fluid mixing and filtration. Furthermore, this flow system is of potential importance for development of bio-separators employing Taylor vortices for enhancement of mass transfer. The fluid flowing in the annular gap between two rotating cylinders has been used as paradigm for the hydrodynamic stability theory and the transition to turbulence. In this paper, the fluid in an annulus between short concentric cylinders is investigated numerically for a three dimensional viscous and incompressible flow. The inner cylinder rotates freely about a vertical axis through its centre while the outer cylinder is held stationary and oscillating radially. The main purpose is to examine the effect of a pulsatile motion of the outer cylinder on the onset of Taylor vortices in the vicinity of the threshold of transition, i.e., from the laminar Couette flow to the occurrence of Taylor vortex flow. The numerical results obtained here show significant topological changes on the Taylor vortices. In addition, the active control deeply affects the occurrence of the first instability. It is established that the appearance of the Taylor vortex flow is then substantially delayed with respect to the classical case; flow without control.

Keywords: CFD simulation; Pulsating motion; Finite geometry; Active control; Taylor-vortex flow.

NOMENCLATURE

d	gap width= $R_2 - R_1$	TCF	Taylor Couette Flow
H	height of cylinder	(U, V, W)	radial, axial and azimuthal velocity components
ITa_{c1}	first instability (TVF)	WVF	wavy vortex flow
LCF	laminar Couette Flow	μ	dynamic viscosity
MWVF	Modulated Wavy Vortex Flow	ρ	density
R_1	radius of inner cylinder	η	radius ratio
R_2	radius of outer cylinder	Ω_1	angular velocity of the inner cylinder
(r, θ , z)	radial, axial and azimuthal directions	f	frequency
Ta	Taylor number	ε	oscillating amplitude
Ta_{c2}	second instability (WVF)	$\Gamma = H/d$	aspect ratio
Ta_{c3}	third instability (MWVF)		
TVF	Taylor Vortex Flow		

1. INTRODUCTION

The study of rotating flows has currently attracted many researchers, both fundamental and applied. Among the rotating systems most used, the device called Taylor-Couette plays an important role in the development of various instabilities as well as to its relevance as prototypical flow in the study of laminar-turbulent transition. Indeed, Taylor-Couette

flow is an example of a fluid system which becomes turbulent more gradually than most other fluid flows. This system consisting of the flow in the annular gap between two concentric rotating cylinders has a great wealth especially in the phenomenological analysis of the fundamental physical processes such as: the laminar-turbulent transition, the various industrial applications: tribology, tangential filtration, crystallization,

turbomachinery, mixing processes, liquid-liquid extraction and bio-reaction. Since the pioneering work of Taylor (1923), the rotor-stator configuration has been the subject of numerous studies. In the case of flow between two long cylinders with an outer one stationary, the base flow depends only on the radius. Thus, the various flow regimes occurring in the infinite Taylor-Couette system are well known [Chandrasekhar, (1961); Coles, (1965); Fenstermacher *et al.*, (1979); Diprima and Swinney, (1981); Marcus, (1984); Bouabdallah, (1980); Koschmieder, (1993); Avila *et al.*, (2008); Sobolik *et al.*, (2011); Martinez-Arias *et al.*, (2014); Adnane *et al.*, (2015)]. It is important to note that few references from the extensive literature that has developed in this flow for the large aspect ratio have been cited here.

However, the geometric parameters such as the aspect ratio and the radius ratio have an important role in the transition mechanism to turbulence. Cole, (1976) and Benjamin, (1978a, 1978b) were the first who found that the aspect ratio profoundly affects the flow regimes and the transition to turbulence. Indeed, Cole, (1976) has investigated the effect of finite length cylinders on the occurrence of the Taylor vortex flow and wavy vortex flow. He showed that the appearance of the Taylor vortices occurs for a critical Taylor number very close to the critical value of the classical case (infinitely rotating cylinders). In contrast, He found that the Taylor number for the onset of wavy mode increases when the cylinders length are reduced. Further, Benjamin, (1978a) has also described series of the experiments in cylinders of very short length with fixed end plates. He indicated that the bottom and top ends of the cylinders have significant effects on the flow patterns. Furthermore, Alziary de Roquefort and Grillaud, (1978) have employed a finite difference method to analyze the flow behavior in finite length annulus, $\Gamma=10$. They noted that the cellular vortices appear in the vicinity of the mid-plane and that for Re/Re_c between 0.97 and 1.17 the vortex intensity increased rapidly. Indeed, Benjamin and Mullin (1981) found a state of the flow structures which termed the anomalous modes that only exist in the finite Taylor-Couette system.

In addition, Bielek and Koschmieder, (1990) have investigated experimentally the onset of Taylor vortices in finite length cylinders for various aspect ratios ranging from 3 until 3.75. They found that the length of fluid column has a profound effect on the formation and number of the Taylor vortices.

Furthermore, the flow behavior in the short cylinders has been the subject of numerous theoretical, experimental and numerical studies (Hall, (1982); Lücke *et al.*, (1984); Aitta *et al.*, (1985); Heinrichs *et al.*, (1986); Pfister *et al.*, (1988); Nakamura *et al.*, (1990, 1989); Cliffe *et al.*, (1992); Toya *et al.*, (1994); Linek and Ahlers, (1998); Mullin *et al.*, (2002); Czarny *et al.*, (2002); Furusawa *et al.*, (2002); Lopez and Marques, (2003); Watanabe and Toya, 2012). Recently, Deng *et al.*, (2009) presented an experimental and numerical study on the onset of Taylor vortices in short cylinders with an aspect ratio of 5.17. They

found that the vortex number decreases with decreasing fluid column length.

On the other hand, the stabilization of the Taylor-Couette flow has been the subject of the several investigations in order to shifting the threshold of the onset of Taylor vortex flow to larger Taylor numbers. In addition, the superposition of an axial flow, known as Taylor-Couette-Poiseuille flow, has been used as an efficient mechanism to stabilize the basic flow (Snyder, (1962); Meseguer and Marques, (2002); Campero and Vigil, (1999); Poncet *et al.*, (2014)).

Indeed, in order to highlight the new progress in rotating and vortex shedding, Awasthi *et al.*, (2014) have used viscous potential flow theory to analyze the Rayleigh-Taylor instability in the presence of tangential electric field. They showed that the electric field has a stabilizing effect on the considered system. In addition, Yadav *et al.* (2011, 2013) have investigated the thermal instability problem for rotating nanofluid layer using linear stability theory.

The axial oscillation of the inner cylinder has been also used as a stabilization strategy of Taylor-Couette flow. Since, the seminal work of Ludwig, (1964), the effect of the oscillation on the onset of Taylor vortices has received potential interests, both fundamental and applied (Donnelly, (1964); Barenghi and Jones, (1989); Hu and Kelly, (1995); Weisberg *et al.*, (1997); Marques and Lopez, (1997, 2000); Youd *et al.*, (2003, 2005); Sinha *et al.*, (2006)). These authors have shown that oscillations retarded the onset of Taylor vortices to a high angular velocity. More recently, Oualli *et al.*, (2013) have investigated numerically the effect of radial oscillation of the outer cylinder on the laminar turbulent transition in the infinite length cylinders. They found that this control strategy had a stabilizing effect.

The motivation of this numerical study, in addition to its direct connection with the classical Taylor-Couette problem, is to assess the flow response to the imposed radial oscillating motion. Particular attention is given to the onset of Taylor vortices and flow structures when the system is under an active control. The transition phenomena that appear in this flow are discussed under the combined effects of the cylinders height and the radial oscillation of outer cylinder. The computational domain is changed in time due to the different oscillating amplitudes.

2. GOVERNING EQUATIONS AND NUMERICAL MODELING

2.1 Governing Equations

Consider the familiar problem of the motion of a viscous fluid in an annular gap, bounded by two concentric finite cylinders and two parallel end plates fixed to the outer cylinder. The inner cylinder rotates while the outer cylinder and the end walls are stationary, as shown in Fig.1.

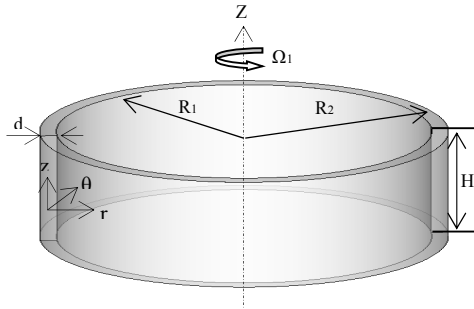


Fig. 1. Finite Taylor Couette geometry.

The dimensionless parameters governing this problem are the ratio of inner to outer radii $\eta=R_1/R_2$, which fixes the geometry of the annulus, the aspect ratio $\Gamma=H/d$ corresponding to the cylinder height reported to the gap and the Taylor numbers.

Where R_1 and R_2 , are respectively the radii of the inner and outer cylinders, Ω_1 is the angular velocity of the inner cylinder, ν is the kinematic viscosity and $d = R_2 - R_1$ is the gap between cylinders.

The flow is described by the conservation of mass and the Navier–Stokes equations, respectively, written using cylindrical variables (r, θ, z) .

$$r : \frac{D}{Dt}U - \frac{V^2}{r} = -\frac{1}{\rho} \frac{\partial P}{\partial r} + \nu \left[\left(\nabla^2 - \frac{1}{r^2} \right) U - \frac{2}{r^2} \frac{\partial V}{\partial \theta} \right] \quad (1)$$

$$\theta : \frac{D}{Dt}V + \frac{UV}{r} = -\frac{1}{\rho r} \frac{\partial P}{\partial \theta} + \nu \left[\left(\nabla^2 - \frac{1}{r^2} \right) V + \frac{2}{r^2} \frac{\partial U}{\partial \theta} \right] \quad (2)$$

$$z : \frac{D}{Dt}W = -\frac{1}{\rho} \frac{\partial P}{\partial z} + \nu \nabla^2 W \quad (3)$$

$$\frac{1}{r} \frac{\partial}{\partial r} (rU) + \frac{1}{r} \frac{\partial V}{\partial \theta} + \frac{\partial W}{\partial z} = 0 \quad (4)$$

The symbol (D/Dt) stands for a differential operator who represents a total derivative compared to time t , such as:

$$\frac{D}{Dt} = \frac{\partial}{\partial t} + U \frac{\partial}{\partial r} + \frac{V}{r} \frac{\partial}{\partial \theta} + W \frac{\partial}{\partial z} \quad (5)$$

The notation $\Delta = \nabla^2$ is the Laplacien operator in the cylindrical coordinates.

$$\nabla^2 = \frac{\partial^2}{\partial r^2} + \frac{1}{r} \frac{\partial}{\partial r} + \frac{1}{r^2} \frac{\partial^2}{\partial \theta^2} + \frac{\partial^2}{\partial z^2} \quad (6)$$

where (U, V, W) are the velocity components and P is the pressure.

With the following boundary conditions:

$r = R_1, V = R_1 \Omega_1$ and $U = W = 0$ for rotating inner cylinder ;

$r = R_2, U = V = W = 0$ for fixed outer cylinder ;

$z = 0, U = V = W = 0$ for fixed lower endplate ;

$z = H, U = V = W = 0$ for fixed upper endwall.

2.2 Numerical Modeling

The simulations were carried out using axisymmetric 3-D grids. More grid points are taken in the axial and radial directions compared with the azimuthal direction because there are high shear regions near the inner and outer cylinder walls and the endplates (top and bottom). The number of grid points determined by grid-refinement study was 2073600 hexahedral cells, $(36 \times 360 \times 160)$ in the radial (r) , axial (z) and azimuthal (θ) directions, respectively. The mesh is uniformly distributed in the azimuthal directions but linear condensed in two ends and next to inner and outer wall, as illustrated in Fig 2.

The numerical results are obtained using the simulation code Fluent, based on the finite volume method. The discretization scheme chosen for the pressure is the second order model. The third order MUSCL scheme was used for the moment equations. For the pressure-velocity coupling, the Pressure-Implicit with Splitting of Operators (PISO) algorithm was selected. The time step is fixed equal to $\Delta t = 0.0002$. The maximum number of iterations by time step is 1000 iterations. The convergence criteria are based on the residuals value. The converged solution is assumed when all residuals are less than 10^{-6} . The oscillation of the outer cylinder is done by a dynamic mesh model where the shape of the domain changes with time. For this, a predefined function, user defined function (UDF), is used to change the shape of the grid cells; create and eliminate the cells to ensure the desired pulsatile motion.

The present numerical results, concerning the first and second instability, are compared and validated against other works for a similar geometry, as shown in Table 1. The computed critical Taylor numbers showing the onset of TVF, agree quite well with other data reported previously in the literature.

3. MAIN RESULTS

3.1 Taylor Couette flow Without Control

3.1.1 Flow Patterns

In this part, we consider the Taylor-Couette flow without control. The various flow regimes obtained in this numerical simulation is shown in figure 3, corresponds to the contours of the pressure field for low values of Taylor until the appearance of the first instability (TVF), the second instability (WVF) then the third instability (MWVF).

Our simulations begin with the laminar Couette flow (LCF), which is the base flow in the absence of any disturbance. This mode can be described as a homogenous movement of high degree of symmetry

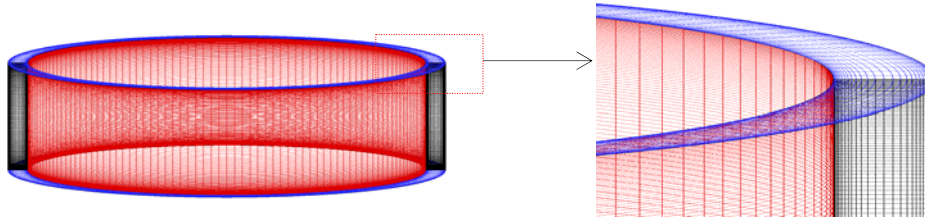


Fig. 2. Grid discretizing the computational domain.

Table 1 Comparison between our numerical results and previous experimental works

Authors Ta	Alziary <i>et al</i> (1978)	Mahamdia <i>et al</i> (2003)	Leng <i>et al</i> (2014)	Our study	Comparison with Mahamdia <i>et al</i>
Ta _{c1}	41.8	42.25	42.5	42	0.6%

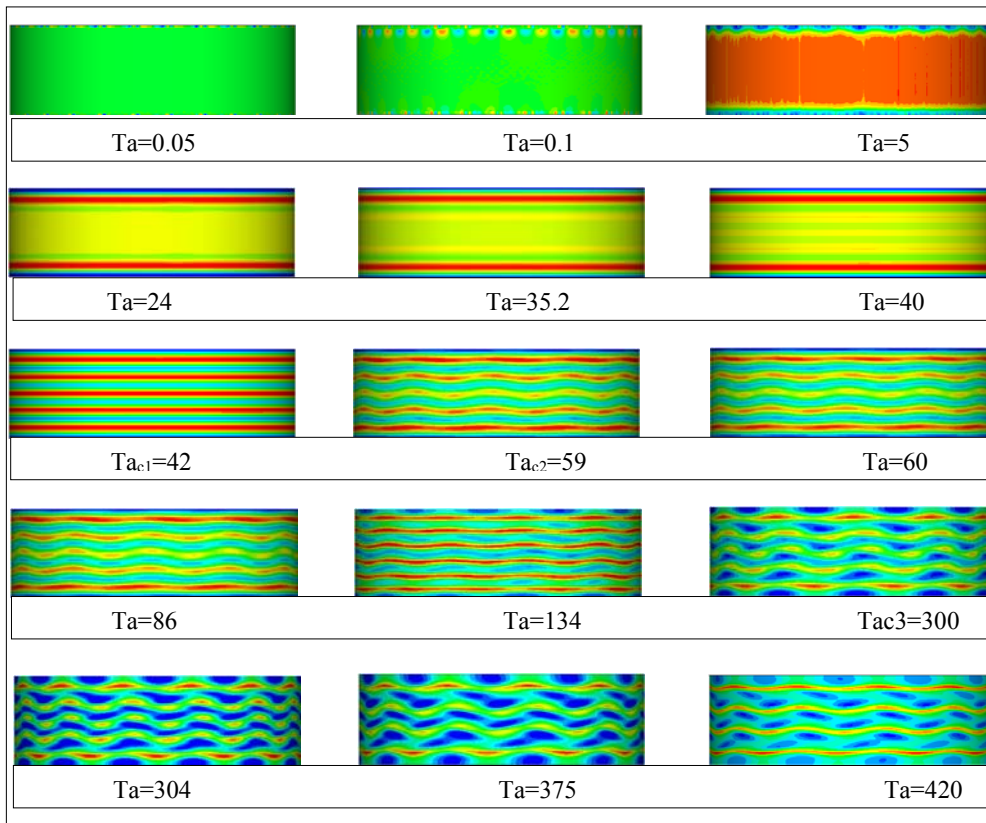


Fig. 3. Various flow regimes in the finite-length geometry

in the fluid. At $Ta=0.1$, the Ekman vortices occur on both endwalls. For $Ta = 5$, we observe vertical lines distributed axially along the wall of the outer cylinder induced by the imbalance between the centrifugal force and the pressure gradient. From $Ta = 35.2$, it can be seen the development of rolls that spread from the endwalls to the middle of the system. Then, when the Taylor number reaches the critical value, $Ta_{c1}=42$, we observe the appearance of five rolls representing the first stage of the laminar-turbulent transition, termed Taylor vortex flow (TVF). Hence, this first instability is steady state and periodic in the axial direction. Furthermore, we note that the Taylor number for the

onset of TVF in the short length cylinders is found very close to the critical Taylor number for the infinite cylinder problem. As the angular velocity of the inner cylinder is increased, a second critical Taylor number Ta_{c2} is reached at which the axisymmetric Taylor vortex flow becomes unstable and a rotating wave appears in the flow. This state, known as wavy vortex flow, is time-periodic and breaks the continuous rotational symmetry. Therefore, there is a transition from time-independent Taylor vortex flow to a time-dependent wavy vortex flow, which consists of the transverse travelling waves superimposed on the horizontal vortices. Indeed, we observe an azimuthal wave

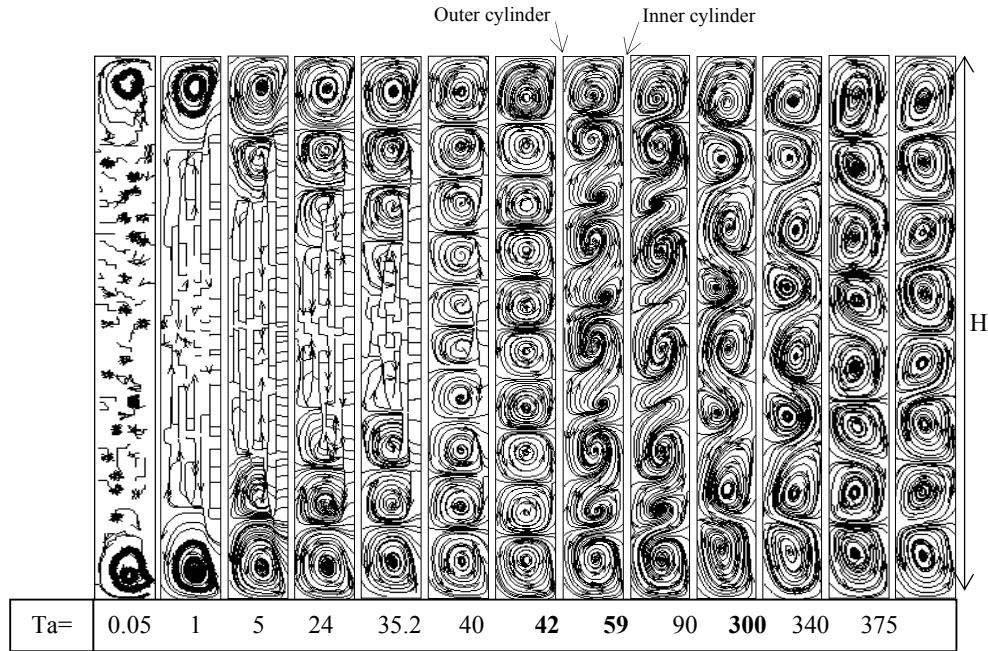


Fig. 4. Formation of the various flow regimes/ streamlines in (r,z) plane.

train rotates about the axis (oz) and propagating in the azimuthal (θ) direction. We note that the Taylor number at which the wavy vortex flow occurs in the finite cylinders, $Ta_{c2}=59$, is increased considerably compared to the critical Taylor number for the infinite length problem ($Ta=48$).

When the Taylor number becomes larger, an additional wave mode appears which modulates the WVF, as shown in figure 3 at $Ta_{c3}=300$. This flow state is termed the modulated wavy vortex flow (MWF).

3.1.2 Formation Processes of Taylor Cells

Figure 4 depicts the flow structures obtained by representation of computed streamlines in (r, z) plane for several Taylor number, showing the formation mechanism of various flow modes that occur in the finite Taylor-Couette geometry. For a very low angular velocity, small vortices begin to appear near both end walls (top and bottom) in the form of circular cells, known as Ekman vortices. However, the middle of the region is free of the vortices. The vortices developed from the end-boundaries, by the Ekman pumping, induced the formation of next vortices that propagate toward the center of fluid column which can be seen at $Ta = 35.2$. As Taylor number is further increased, the cells propagate towards the center region until it fills completely the fluid column when Taylor number reaches the critical value, $Ta_{c1}= 42$, in which 10 vortices form along the axis of rotation showing a good overall agreement with the numerical results of Alziary de Roquefort and Grillaud, (1978) and Leng *et al.*, (2014) for the same geometrical parameters. When the Taylor number reaches the critical value, $Ta_{c2}=59$, the cells

begin to oscillate in the circumferential direction corresponding to the onset of wavy mode (WVF). Further, the adjacent vortices are not independent and the waves have an S-shape. In addition, there is a tightening in the outflow zone and a stretching in the inflow zone. This is, probably, due to the exchange of momentum between the adjacent cells. Hence, the exchange of fluid between contiguous vortices increases with increasing of the values of Taylor number (more important in inflow than in outflow). From $Ta_{c3} = 300$, we can see the modulation of vortices that announces the occurrence of the modulated wavy vortex flow (MWF). Beyond the onset of MWVF, the vortices periodically oscillate from the S-shape to the flattened shape.

3.2 Taylor-Couette Flow under Active Control

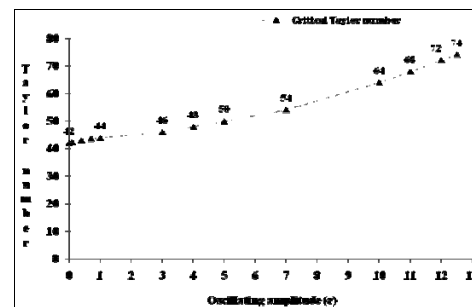


Fig. 5. Critical Taylor number versus oscillating amplitude (ϵ).

The aim of this part is to investigate the response of

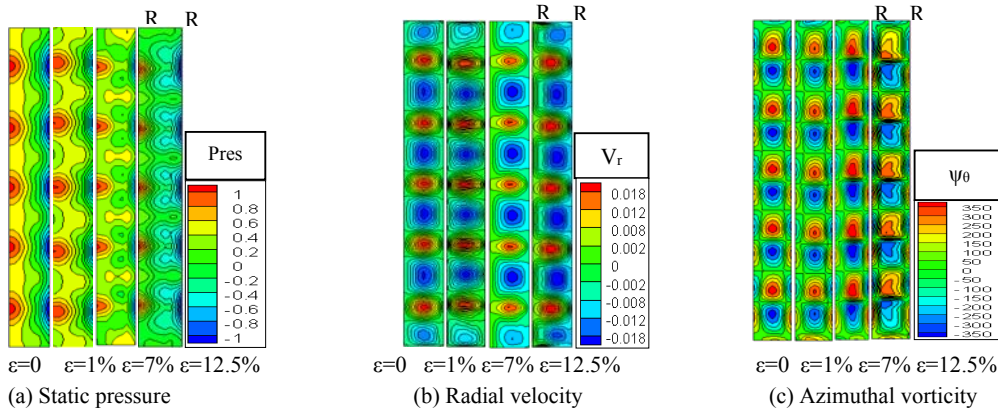


Fig. 6. Configuring of the Taylor Couette flow in the (r, z) plane / First instability.

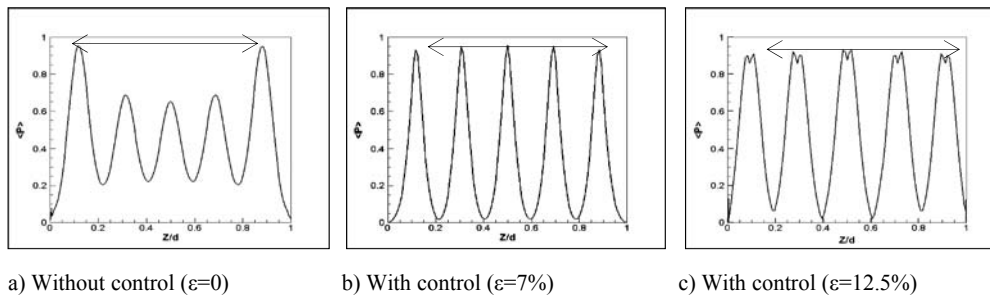


Fig. 7. Mean pressure versus axial position for different oscillating amplitudes ϵ .

the Taylor Couette flow to an active control. The controlled flow is executed by varying the outer cylinder cross section in a sinusoidal movement as follow:

$$r = R_2(1 + \epsilon |\sin 2\pi ft|) \quad (7)$$

when ϵ is oscillating amplitude ($\epsilon = \Delta r/R_2$) and f is the frequency.

The numerical calculations are carried out over a range of oscillating amplitude from 0 until 12.5%. The flow without control corresponds to $\epsilon=0$. The frequency of oscillation is kept fix at the value $f = 50$ Hz.

3.2.1 Variation of the Critical Taylor Number

Figure 3 shows the variation of the critical Taylor number, Ta_{c1} , versus the oscillating amplitudes. It is noticed that the critical Taylor number, characterizing the onset of Taylor vortex flow, increases drastically when the oscillating amplitude increases. For the nominal case, $\epsilon=0$, $Ta_{c1}=42$ and when the value of ϵ reaches 12.5% the Ta_{c1} increases rapidly up to 74. Therefore, the onset of Taylor vortex flow is substantially delayed with respect to natural case. We note that the increase of Taylor number is observed for the entire range of the applied deforming amplitudes from 0.1 to 12.5%. Therefore, the radial oscillation of the outer cylinder has a stabilizing effect on the onset of the

first instability: the relaminarization phenomenon.

3.2.2 Flow Structures

Figure 6 shows contours of static pressure, radial velocity and azimuthal vorticity, respectively in (r,z) plane for some oscillating amplitudes. It is observed that the pulsating motions applied to the Taylor Couette flow have a significant effect on the flow structures, resulting by substantial modifications in the vortices shape. Gradually as the amplitude of oscillation increases, the cell size decreases in which the circular shape of the vortex becomes elliptical. We note, also, the appearance of three different zones; blue zones, characterizing the low speed, move towards the outer cylinder while red zones, characterizing the high speed, localize near the inner cylinder with the occurrence of a green intermediate zone between the two preceding zones similar to an axial jet, as illustrated in fig.6 (b). In addition, the flow behavior can also be seen in figure 7, showing the distribution of the mean pressure component in the middle of the gap plotted against axial position, for the nominal case and two oscillating amplitudes, $\epsilon = 7\%$ and 12.5% , respectively. For the flow without control, $\epsilon = 0$, there are two wide peaks in the curve correspond to the Ekman vortices at the top and bottom end walls. In contrast, when the flow is under active control, $\epsilon \neq 0$, all vortices have the same shape. Thus, from the profile of mean pressure, it is clearly seen that the flow is still symmetric whatever the amplitude of

oscillation applied.

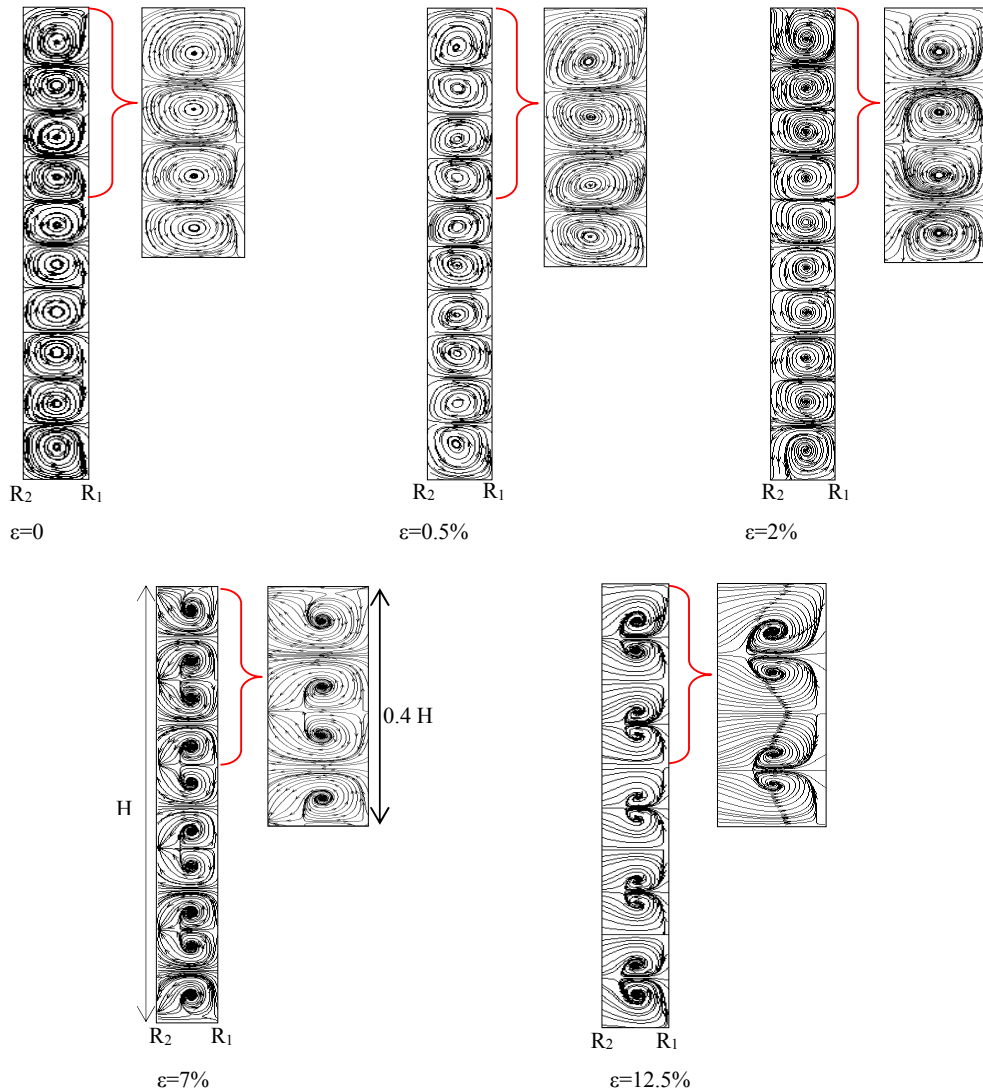


Fig. 8. Taylor vortices structures for different oscillating amplitudes / Streamline in the (r,z) plane.

3.2.3 Behaviour of the Taylor Vortices

We report in fig.8, the computed streamlines in the annulus, representing the projection of the flow in the (r, z) plane, which has allowed us to highlight the following observations:

- For the flow without control, $\epsilon=0$, there are ten cells inside the annulus, each cell rotates in the opposite direction with the adjacent cell. The cells are separated by radial jets of angular momentum emanating from the cylinders boundary layers [49]. This flow pattern is steady and periodic in the axial direction. Each pair of cells has an axial wavelength $\Lambda=2d$.
- For a low amplitude, $\epsilon=0.5\%$, the cells are slightly inclined relative to the vertical axis and stretched radially.
- For a medium amplitude, $\epsilon=2\%$, the cells shape is changed to become oval and elongated in the axial direction. Thus, we see that the two adjacent cells is gathered in the same housing forming a doublet stable similar to the recirculating eddies behind a fixed cylinder placed on a uniform stream at small Reynolds number ($5 < Re < 40$); known as Föppl vortices, Melkounian and Protas, (2014).
- For high amplitudes, $\epsilon \geq 7\%$, the vortices lose their circular form and the flow shows a similar configuration to the flow behind a circular disc in a uniform flow, Yang *et al.*, (2014) and, Krasny and Nitsche, (2002).

4. CONCLUSION

In this paper, we have investigated the Taylor-

Couette problem in a finite geometry under an active control. The viscous incompressible fluid between two rotating cylinders was simulated using a three-dimensional CFD code, with the inner cylinder rotates with a constant angular velocity while the outer one is stationary and subject to pulsatile motion. For the nominal case (without control), the flow regimes encountered through this study when the Reynolds number is increased stepwise are: laminar Couette flow, Taylor-vortex flow, wavy vortex flow and modulated wavy vortex flow. However, in the controlled case, the radial oscillation of outer cylinder profoundly affects the flow behavior and leads to significant topological changes in the Taylor vortices. In addition, the controlling strategy led to a significant flow relaminarization; the occurrence of Taylor vortex flow is considerably delayed. The stabilization of Taylor Couette flow has direct applications to centrifugal pumps and lubrication problems when laminar flow regime is desired. Furthermore, this strategy of flow control remains important in the tribology in order to establish the optimum conditions for the lubrication of bearings transmission speeds in the automotive industry, aeronautics and plants producing electricity.

REFERENCES

- Adnane, E., A. Lalaoua and A. Bouabdallah (2015). An experimental study of the laminar – turbulent transition in a tilted Taylor-Couette system subject to free surface effect. *Journal of Applied Fluid Mechanics* 9(3), 1097-1104, 2016.
- Aitta, A., G. Ahlers and D. S. Cannel (1985). Tricritical Phenomena in Rotating Couette-Taylor Flow. *Phys. Rev. Lett.* 54, 673–676.
- Alziary de Roquefort, T., G. Grillaud (1978). Computation of Taylor vortex flow by a transient implicit method. *Comput. Fluids* 6, 259-269.
- Avila, M., M. Grimes, J. M. Lopez and F. Marques (2008). Global endwall effects on centrifugally stable flows. *Phys. Fluids* 20, 104104.
- Awasthi, M. K., D. Yadav and G. S. Agrawal (2014). Viscous potential flow analysis of Electro hydrodynamic Rayleigh-Taylor instability International. *Journal of Applied Mathematics and Mechanics.* 7, 209-216.
- Barenghi, C. F. and C. A. Jones (1989). Modulated Taylor-Couette flow. *J. Fluid Mech.* 208, 127-160.
- Benjamin, T. B. (1978). Bifurcation Phenomena in Steady Flows of a Viscous Fluid: I. Theory. *Proceedings of the Royal Society* 359, 1-26.
- Benjamin, T. B. (1978). Bifurcation Phenomena in Steady Flows of a Viscous Fluid: II. Experiments. *Proceedings of the Royal Society, A* 359, 27-43.
- Benjamin, T. B. and T. Mullin (1981). Anomalous modes in the Taylor experiment. *Proc. Roy. Soc. London* 377, 221–249.
- Bielek, C. A. and E. L. Koschmieder (1990). Taylor vortices in short fluid columns with large radius ratio. *Phys. Fluids* 2, 1557.
- Bouabdallah, A. and G. Cognet (1980). Laminar-turbulent transition in Taylor-Couette flow. In: *Laminar Turbulent Transition (IUTAM Conference)*, edited by R. Eppler and H. Fasel (Springer-Verlag, Berlin). 368-377.
- Campero, R. J. and R. D. Vigil (1999). Flow Patterns in Liquid-Liquid Taylor-Couette-Poiseuille Flow. *Ind. Eng. Chem. Res.* 38, 1094-1098.
- Chandrasekhar, S. (1961). *Hydrodynamic and Hydromagnetic Stability*. Oxford at the Clarkndon Press.
- Cliffe, K. A., J. J. Kobine and T. Mullin (1992). The Role of Anomalous Modes in Taylor–Couette Flow. *Int. J. Heat Mass Transfer* 439, 341–357.
- Cole, J. A. (1976). Taylor- vortex instability and annulus- length effects. *J.Fluid. Mech* 75, 5-12.
- Coles, D. (1965). Transition in Circular Couette Flow. *J. Fluid Mech* 21, 385-425.
- Czarny, O., E. Serre, P. Bontoux and R. M. Lueptow (2002). Spiral and wavy vortex flows in short counter-rotating Taylor-Couette cells, Theoret. Comput. *Fluid Dynamics* 16, 5-15.
- Deng, R., D. Y. Arifin, Y. C. Mak and C. H. Wang (2009). Characterization of Taylor vortex flow in a short liquid column. *AIChE Journal* 55, 3056-3064.
- Diprima, R. C. and H. L. Swinney (1981). *Instabilities and transition in flow between concentric rotating cylinders.* In: *Hydrodynamic Instabilities and the Transition to Turbulence* (ed. H. L. Swinney and J. P. Gollub) Springer, 139-180.
- Donnelly, R. J. (1964). Experiments on the stability of viscous flow between rotating cylinders. III enhancement of stability by modulation. *Proc. Roy. Soc. Lond.A* 281, 130-139.
- Fenstermacher, P. R., H. L. Swinney and J. P. Gollub (1979). Dynamical instabilities and the transition to chaotic Taylor vortex flow. *J. Fluid Mech* 94, 103-128.
- Furusawa, H., T. Watanabe, Y. Toya and I. Nakamura (2002). Flow pattern exchange in the Taylor-Couette system with a very small aspect ratio. *Phys. Rev. E* 65, 036306–036312.
- Hall, P. (1982). Centrifugal instabilities of circumferential flows in finite cylinders: the wide gap problem. *Proc. Roy. Soc. London,* 384, 359–379.
- Heinrichs, R., G. Ahlers and D. S. Cannel (1986).

- Effects of Finite Geometry on the Wave Number of Taylor-Vortex Flow. *Phys. Rev. Lett.* 56, 1794–1797.
- Hu, H. C. and R. E. Kelly (1995). Effect of a time-periodic axial shear flow upon the onset of Taylor vortices. *Phys. Rev. E* 51, 3242-3251.
- Koschmieder, E. L. (1993). *Benard cells and Taylor vortices*. Cambridge University Press, NewYork.
- Krasny, R. and M. Nitsche (2002). The onset of chaos in vortex sheet flow. *J. Fluid. Mech.* 454, 47–69.
- Leng, X. Y., Y. Yu and B. W. Li (2014). Numerical study of MHD Taylor vortex flow with low magnetic Reynolds number in finite-length annulus under uniform magnetic field. *Computers and Fluids* 105, 16-27.
- Linek, M. and G. Ahlers (1998). Boundary Limitation of Wave Numbers in Taylor-vortex Flow. *Phy. Rev. E* 58, 3168-3174.
- Lopez J. M. and F. Marques (2003). Small aspect ratio Taylor–Couette flow: Onset of a very-low-frequency three-torus state. *Phys. Rev. E* 68, 1036302.
- Lücke, M., M. Mihlicic and K. Wingerath (1984). Flow in small annulus between concentric cylinders. *J. Fluid Mech* 140, 343–353.
- Ludwig, H. (1964). Experimentelle Nachprüfung des Stabilitätstheorien für reibungsfreie Strömungen mit schraubenlinienförmigen Stromlinien. *Z. Flugwiss* 12, 304–309.
- Mahamdia, A., A. Bouabdallah and S. E. Skali (2003). Effets de la surface libre et du rapport d'aspect sur la transition de l'écoulement de taylor-couette. *C. R. Mécanique* (331), 245–252.
- Marc, A. C. (2008). *Nonlinear dynamics of mode competition in annular flows*. Ph.D. Thesis, Universitat Politècnica de Catalunya.
- Marcus, P. S. (1984). Simulation of Taylor–Couette flow. Numerical methods and comparison with experiment. *J. Fluid Mech* 146, 45-64.
- Marques, F. and J. M. Lopez (1997). Taylor-Couette flow with axial oscillations of the inner cylinder: Floquet analysis of the basic flow. *J. Fluid Mech.* 348, 153-175.
- Marques F. and J. M. Lopez (2000). Spatial and temporal resonances in a periodically forced hydrodynamic system. *Phys. D* 136(3-4), 340-352.
- Martinez-Arias, B., J. Peixinho, O. Crumeyrolle and I. Mutabazi (2014). Effect of the number of vortices on the torque scaling in Taylor-Couette flow. *J. Fluid. Mech* 748, 756- 767.
- Melkounian, S. and B. Protas (2014). Wake Effects on drift in two-dimensional inviscid incompressible flows. *Phy. Fluids* 26, 123601.
- Meseguer, A. and F. Marques (2002). On the competition between centrifugal and shear instability in spiral Poiseuille flow. *J. Fluid. Mech.* 455, 129-148.
- Mullin, T., Y. Toya and S. J. Tavener (2002). Symmetry breaking and multiplicity of states in small aspect ratio Taylor–Couette flow. *Phys. Fluids* 14, 2778-2787.
- Nakamura, I., Y. Toya, S. Yamashita and S. Ueki (1989). An experiment on a Taylor Vortex Flow in a Gap with a Small Aspect Ratio (Instability of Taylor Vortex Flows). *JSME International Journal. Series II* 23, 388-394.
- Nakamura, I., Y. Toya, S. Yamashita and Y. Ueki (1990). An Experiment on a Taylor Vortex Flow in a Gap with a Small Aspect Ratio (Bifurcation of Flows in a Symmetric System). *JSME International Journal. Series II* 33, 685-691.
- Oualli, H., A. Lalaoua, S. Hanchi and A. Bouabdallah (2013). Taylor-Couette flow control using the outer cylinder cross-section variation strategy. *Eur. Phys. J. Appl. Phys.* 61, 11102.
- Pfister, G., H. Schmidt, K. A. Cliffe and T. Mullin (1988). Bifurcation phenomena in Taylor–Couette flow in a very short annulus. *J. Fluid. Mech* 191, 1-18.
- Poncet, S., S. Viazzo and R. Oguic (2014). Large eddy simulations of Taylor-Couette-Poiseuille flows in a narrow-gap system. *Phys. Fluids* 26, 105108.
- Sinha, M., I. G. Kevrekidis and A. J. Smits (2006). Experimental study of a Neimark- Sacker bifurcation in axially forced Taylor-Couette flow. *J. Fluid Mech.* 558, 1-32.
- Snyder, H. A. (1962). Experiments on the stability of spiral flow at low axial Reynolds numbers. *Proc. Roy. Soc. Lond. A* 265, 198–214.
- Sobolik, V., T. Jirout, J. Havlica and M. Kristiawan (2011). Wall Shear Rates in Taylor Vortex Flow. *JAFM* 2(4), 25-31.
- Taylor, G. (1923). Stability of a viscous liquid contained between two rotating cylinders. *Philos. Trans. Roy. Soc. Lond.*, 223, 289-343.
- Toya, Y., I. Nakamura, S. Yamashita and S. Ueki (1994). An Experiment on a Taylor Vortex Flow in a Gap with a Small Aspect Ratio: Bifurcation of Flows in an Asymmetric system. *Acta Mechanica* 102, 137-148.
- Watanabe, T. and Y. Toya (2012). Vertical Taylor-Couette Flow with Free Surface at Small Aspect Ratio. *Acta Mechanica* 222, 347-353.
- Weisberg, A. Y., I. G. Kevrekidis and A. J. Smits (1997). Delaying transition in Taylor-Couette flow with axial motion of the inner cylinder. *J. Fluid Mech.* 348, 141-151.
- Yadav, D., G. S. Agrawal, R. Bhargava (2011).

- Thermal instability of rotating nanofluid layer. *Int J Eng Sci.* 49, 1171–84.
- Yadav, D., G. S. Agrawal and R. Bhargava (2013). Numerical solution of a thermal instability problem in a rotating nanofluid layer. *Int J Heat Mass Transfer.* 63, 313–22.
- Yang, J., M. Liu, G. Wu, W. Zhong and X. Zhang (2014). Numerical study on instabilities behind a circular disk in a uniform flow. *Int. J. Heat and Fluid Flow* 50, 359–368.
- Youd, A. J., A. P. Willis and C. F. Barenghi (2005). Non-reversing modulated Taylor-Couette flows. *Fluid Dynam. Res.* 36, 61-73.
- Youd, A. J., A. P. Willis and C. F. Barenghi (2003). Reversing and non-reversing modulated Taylor-Couette flow. *J. Fluid Mech.* 487, 367-376.